Supercond. Sci. Technol. **25** (2012) 045012 (6pp) doi:10.1088/0953-2048/25/4/045012

Effect of rare-earth composition on microstructure and pinning properties of Zr-doped (Gd, Y)$Ba_2Cu_3O_x$ superconducting tapes

V Selvamanickam[1], Y Chen[2], Y Zhang[1], A Guevara[1], T Shi[1], Y Yao[1], G Majkic[1], C Lei[2], E Galtsyan[1] and D J Miller[3]

[1] Department of Mechanical Engineering and Texas Center for Superconductivity, University of Houston, Houston, TX 77204, USA
[2] SuperPower Inc, Schenectady, NY 12304, USA
[3] Electron Microscopy Center and Materials Science Division, Argonne National Laboratory, Argonne, IL 60439, USA

Received 21 December 2011, in final form 30 January 2012
Published 12 March 2012
Online at stacks.iop.org/SUST/25/045012

Abstract
The effect of changing Gd + Y content from 1.2 to 1.6 in the precursor of (Gd, Y)$Ba_2Cu_3O_7$ superconducting thin film tapes made by metal organic chemical vapor deposition (MOCVD) at a constant Gd:Y ratio and a fixed Zr content of 7.5% has been studied. The influence of changing the Gd:Y ratio from Gd = 0 to Y = 0 in 0.2 mol steps at a constant Gd + Y content of 1.2 in the precursor has also been investigated at a fixed Zr content of 7.5%. The critical current of these films is found to vary significantly as a function of rare-earth content as well as a function of rare-earth type. Even for a fixed Zr content, it is found that the critical current in the orientation of magnetic field parallel to the *a–b* plane and that in the orientation of field perpendicular to the *a–b* plane can be systematically varied with changing Gd + Y content as well as with changing Gd:Y ratio. The nanoscale defect structures along the *a–b* plane and along the *c*-axis are found to be sensitive to these changes in rare-earth content and type.

(Some figures may appear in colour only in the online journal)

1. Introduction

Thin film high temperature superconducting (HTS) tapes made by reel-to-reel continuous processing are now produced in industry in lengths of more than a kilometer [1]. The enabling technology for high performance HTS tapes is epitaxial growth of the superconducting film on a flexible, inexpensive, polycrystalline metal substrate with intermediate buffer layers. A number of techniques have been used to deposit the superconducting film to produce long thin film HTS tapes, including metal organic chemical vapor deposition (MOCVD) [1], pulsed laser deposition (PLD) [2] and metal organic deposition (MOD) [3]. It is remarkable that epitaxial growth can be maintained even at deposition rates of 0.5 μm min^{-1} in processes such as MOCVD to fabricate thin film HTS tapes. Critical current densities (J_c) as high as 6–7 MA cm^{-2} have been demonstrated in short lengths of superconducting films on a flexible substrate, which are comparable to those achieved in films on single crystal substrates [4]. While such high current densities are noteworthy, a major challenge in the use of HTS tapes in many applications is the significant reduction of the critical current density in the presence of a magnetic field. Over the past six years, significant progress has been made in engineering nanoscale defects in the superconducting film *in situ* during the epitaxial growth process which have contributed to a doubling of critical current (I_c) in the presence of a magnetic field [5, 6]. Such defects have been typically perovskites, such as $BaZrO_3$ (BZO) [7–11] and $BaSnO_3$ [12], pyrochlores, such as Gd_3TaO_7 [13], and double perovskites, such as

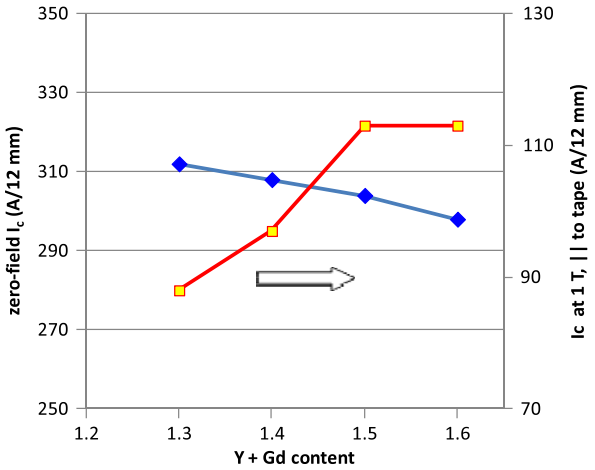

Figure 1. Influence of rare-earth content on the critical current of 7.5% Zr-doped (Gd, Y)BCO superconducting tapes at 77 K in zero field and at 1 T applied parallel to the tape surface.

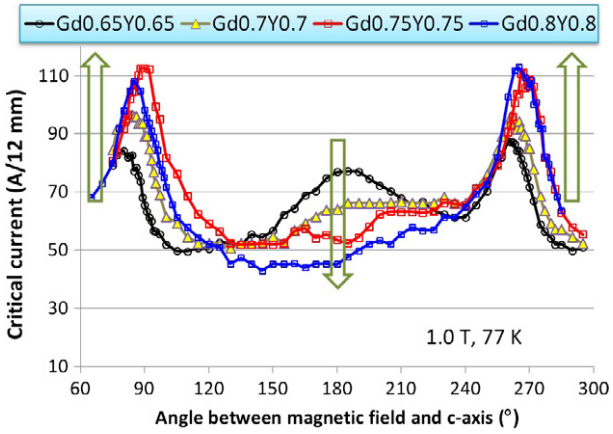

Figure 2. Influence of rare-earth content on the angular dependence of critical current of 7.5% Zr-doped (Gd, Y)BCO superconducting tapes at 77 K at 1 T.

Ba_2YNbO_6 [14, 15]. In most cases, the materials used as engineered defects consist of cations chemically compatible with superconducting $REBa_2Cu_3O_7$ (RE = rare earth). In the case of *in situ* superconductor processing techniques such as MOCVD [5, 6] and PLD [7–10, 12–15], these defects grow primarily normal to the plane of the film by a self-assembly process and in the case of *ex situ* processing techniques, they are added as nanoparticles to the precursor [11]. While a number of groups have reported results on engineered defects by addition of dopants such as those mentioned above, there has not been a systematic work on the influence of rare-earth content and type in the superconductor on the microstructure and flux pinning properties of thin film superconducting tapes made with the addition of dopants that have contributed to improved pinning. The motivation of our work was to examine the influence of rare-earth content and type in (Gd, Y)$Ba_2Cu_3O_7$ films made with Zr addition.

2. Experimental details

All (Gd, Y)BaCuO films made in this work were made in a reel-to-reel continuous MOCVD process [16]. Hastelloy C-276 substrates, 50 μm in thickness and 12 mm in width with a multilayer oxide buffer architecture were used. Biaxial texture that is essential to achieve high critical current densities was achieved in an intermediate MgO layer using ion beam assisted deposition (IBAD) [17]. The superconducting films were grown atop a $LaMnO_3$ layer that was grown epitaxially on the MgO [18]. Previously, we had found that 7.5 at.% Zr addition yielded the best in-field critical current density at 77 K [5]. Hence this level of Zr addition was used in all samples made in this work.

In the first set of samples, the mole contents of Gd and Y were maintained equal and the total rare content in the precursor was modified as $(GdY)_{1.3}$, $(GdY)_{1.4}$, $(GdY)_{1.5}$, and $(GdY)_{1.6}$. The Ba and Cu content in the precursor and a HTS film thickness of 0.5 μm were maintained the same in all cases. In the second set of samples, the total rare-earth content in the precursor was maintained at $(GdY)_{1.2}$ and the Gd:Y mole ratio was modified as 1.2:0, 1:0.2, 0.8:0.4, 0.6:0.6, 0.4:0.8, 0.2:1, and 0:1.2. Therefore, the precursor composition was varied from 100% GdBCO to 100% YBCO in 0.2 mol increments. For these samples, a HTS film thickness of 0.5 μm was used.

Transport critical current measurements were conducted at 77 K, in zero applied magnetic field and in the presence of magnetic field up to 1.5 T using the standard four-probe method. The in-field critical current measurement was performed in the orientation of magnetic field parallel as well as perpendicular to the film normal. Additionally, the angular dependence of critical current was measured at 1 T and 77 K over an angular range of 220° to the wire axis. Cross sectional transmission electron microscopy (TEM) and focused ion beam–scanning electron microscopy (FIB–SEM) examination of a few samples were conducted to examine the morphology, orientation, and size of nanoscale defects created in the films.

3. Results and discussion

The critical currents of samples made with equal Gd and Y mole content but different rare-earth content measured at 77 K and zero applied magnetic field are shown in figure 1. As shown in the figure, a critical current of all samples with total precursor rare-earth content of 1.3–1.6 was maintained at about 300 A/12 mm width within a spread of only 10 A/12 mm. Figure 2 displays the angular dependence of critical current of the four samples and remarkable differences are seen. The Zr-doped film with a rare content of 1.3 exhibits a pronounced peak in critical current in the orientation of field perpendicular to the film plane, as intense as the peak parallel to the film plane. The critical current retention in a 1 T field perpendicular to the film plane is about 26% of the zero-field value, which is in the typical range observed for Zr-doped films. However, with increasing rare-earth content and even with the same 7.5% Zr value, critical current at 1 T applied perpendicular to the film steadily decreases. In

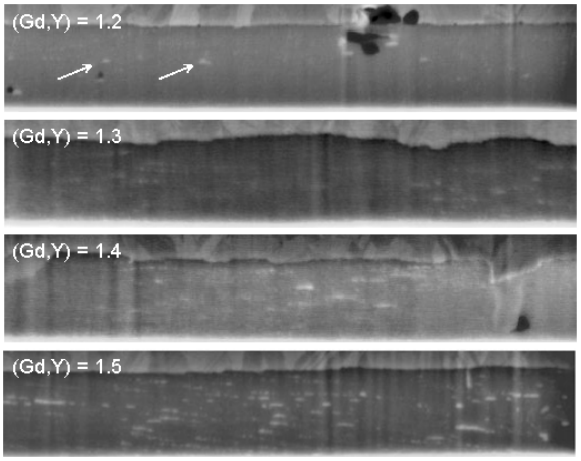

Figure 3. Cross sectional microstructures of 7.5% Zr-doped (Gd, Y)BCO superconducting tapes made with different rare-earth content. Arrows point to rare-earth oxides in the film.

fact, with high rare-earth levels, the peak that is ubiquitously observed in BZO-containing films regardless of the process type (PLD, MOD, MOCVD) is found to disappear completely. On the other hand, as shown in figure 2, as the rare-earth content in the Zr-doped films is increased, the critical current in the field orientation along the film plane increases steadily. These values are included in the plot in figure 1 and it is seen that the critical current at 1 T field applied along the film plane increases by 35% as the precursor rare-earth content is increased from 1.3 to 1.6. Accordingly, the retention of zero-field critical current at 1 T in this field orientation increases from 27% in the sample with rare-earth content of 1.3 to 38% in the sample with rare-earth content of 1.6. In spite of the significant differences in the critical current performance in the orientations of field parallel and perpendicular to the film plane, the minimum critical current is essentially the same in all samples with rare-earth content of 1.3, 1.4, and 1.5. Only the sample with rare content of 1.6 shows a lower minimum I_c.

Cross sectional examination of the microstructures of Zr-doped MOCVD films with different rare-earth content was observed using FIB–SEM and the results are shown in figure 3. As shown in the figure, $(Gd, Y)_2O_3$ nanoprecipitates are found aligned at a shallow angle to the film plane. The inclination arises from the inclination of the *a–b* plane itself in HTS films made using IBAD templates [19] and hence $(Gd, Y)_2O_3$ nanoprecipitates are oriented along the *a–b* plane. It is clearly seen from figure 3 that the density of these nanoprecipitates increases steadily with increasing rare-earth content. It is believed that this increase in the rare-earth oxide precipitate density is responsible for the improved pinning in the orientation of field along the film plane with increasing rare-earth content.

Cross sectional microstructures of Zr-doped samples with $(Gd, Y)_{1.2}$ and $(Gd, Y)_{1.5}$ as observed by TEM are exhibited in figure 4. The microstructure of the $(Gd, Y)_{1.2}$ sample clearly reveals extended self-assembly nanocolumns of BZO along the *c*-axis as well as RE_2O_3 nanoprecipitates along the *a–b* plane. The microstructure of the $(Gd, Y)_{1.5}$ sample shows more abundant RE_2O_3 nanoprecipitates, which is consistent with the FIB observations in figure 3 and also reveals that the BZO nanocolumns are truncated by these precipitates. It is hypothesized that the truncation of the BZO nanocolumns by the RE_2O_3 nanoprecipitates limits the effectiveness of flux pinning in the field orientation along the *c*-axis, leading to a lower critical current in that orientation with increasing rare-earth content in the precursor. It is possible that the shorter BZO nanocolumns are able to pin only short lengths of the vortex lines along the *c*-axis and the unpinned segments are able to move causing dissipation at lower current values.

The results from hereon were obtained from the second set of experiments wherein the total rare-earth content was maintained at 1.2 and the rare-earth type was varied from Gd to Y in 0.2 mol increments. Figure 5 displays the critical current of these samples at 77 K in zero applied magnetic

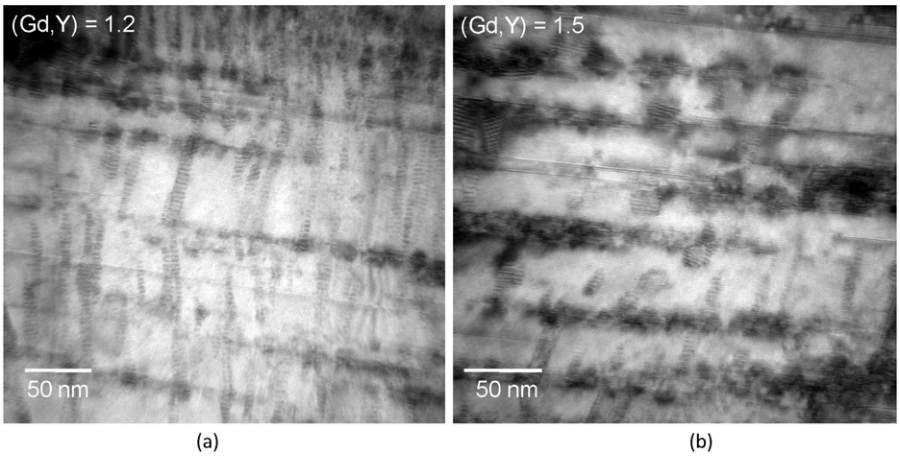

Figure 4. Cross sectional microstructures of 7.5% Zr-doped (Gd, Y)BCO superconducting tapes made with rare-earth content of (a) $(Gd, Y)_{1.2}$ and (b) $(Gd, Y)_{1.5}$ in the precursor.

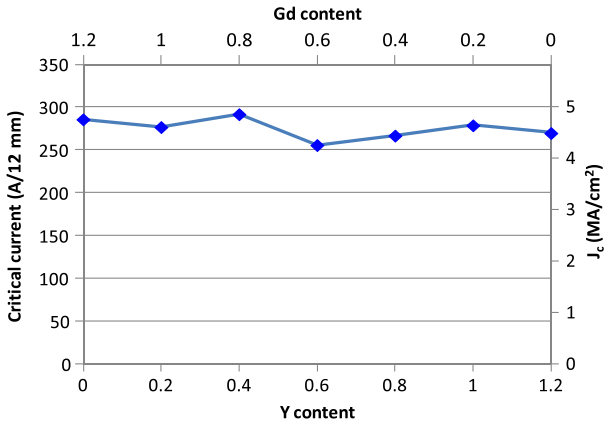

Figure 5. Critical current density of 7.5% Zr-doped (Gd, Y)BCO superconducting tapes made with different ratios of Gd to Y with fixed total rare-earth content of $(Gd, Y)_{1.2}$ in the precursor.

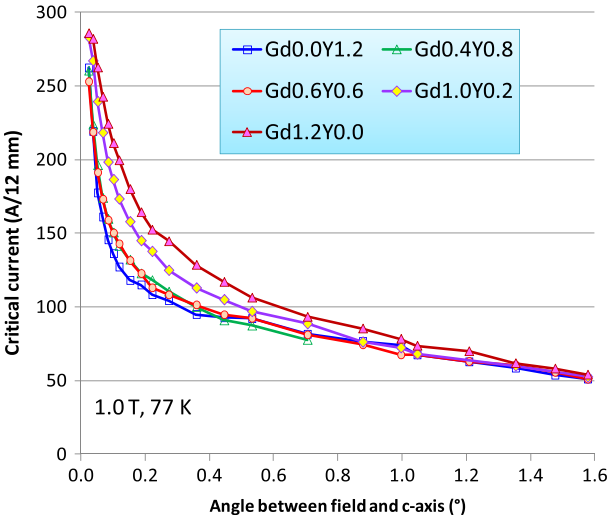

Figure 6. Magnetic field dependence at 77 K with a critical current density of 7.5% Zr-doped (Gd, Y)BCO superconducting tapes made with different ratios of Gd to Y with fixed total rare-earth content of $(Gd, Y)_{1.2}$ in the precursor.

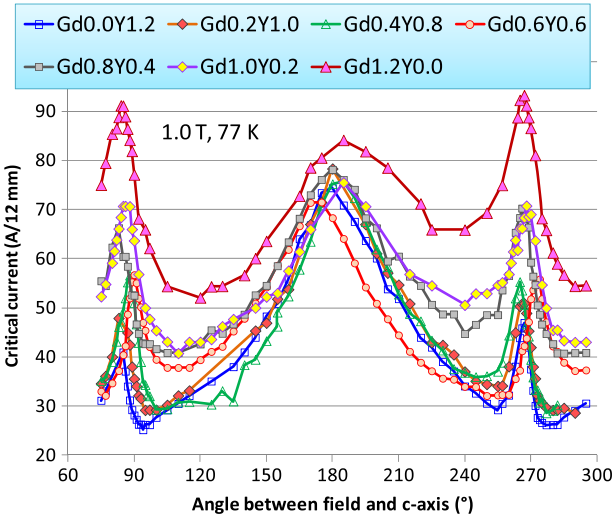

Figure 7. Angular dependence of 77 K, 1 T critical current density of 7.5% Zr-doped (Gd, Y)BCO superconducting tapes made with different ratios of Gd to Y with fixed total rare-earth content of $(Gd, Y)_{1.2}$ in the precursor.

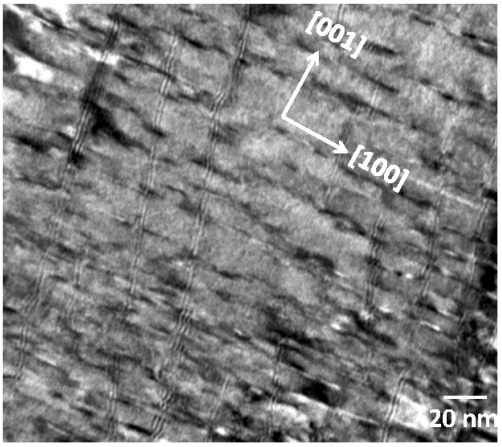

Figure 8. Cross sectional microstructure of 7.5% Zr-doped (Gd, Y)BCO superconducting tape made with rare-earth content of $(Gd_{0.2}Y_{1.0})_{1.2}$ in the precursor.

field. It is evident from the figure that the critical current at zero magnetic field is maintained essentially the same in all seven samples with varying ratio of Gd:Y.

The critical currents of samples with different Gd:Y ratio in increasing magnetic fields applied perpendicular to the film plane are summarized in figure 6. It is seen that the rate of decrease in critical current with increasing magnetic field becomes slower with increasing Gd:Y ratio. For example, in a field of 0.1 T, the critical current of the $Gd_{1.2}Y_{0.0}$ film is 55% and 41% higher than the critical currents of the $Gd_{0.0}Y_{1.2}$ and $Gd_{0.6}Y_{0.6}$ films, respectively. However, the critical currents of the films converge to a similar value in a field of 1 T perpendicular to the film plane. For instance, the critical currents of the $Gd_{1.2}Y_{0.0}$ and $Gd_{0.0}Y_{1.2}$ films at 1 T are within 6% of each other.

Angular dependences of the critical current of the set of samples with different Gd:Y ratios in a field of 1 T are presented in figure 7 and reveal more systematic differences among the samples. As shown in the figure, a prominent peak in the orientation of field perpendicular to the film plane is present in the critical current characteristic of all samples with an almost identical intensity. However, the critical current in the orientation of field parallel to the film plane is found to decrease systematically from the $Gd_{1.2}Y_{0.0}$ film to the $Gd_{0.0}Y_{1.2}$ film. Additionally, the minimum critical current is also found to decrease systematically from the $Gd_{1.2}Y_{0.0}$ film to the $Gd_{0.0}Y_{1.2}$ film.

Analysis of the cross sectional microstructure of $Gd_{0.2}Y_{1.0}$ film was conducted by TEM and the result is shown in figure 8. As the figure shows, extended BZO nanocolumns are seen through the thickness of the film. Defects are observed in the *a*–*b* plane too, but these have not been confirmed to be RE_2O_3 nanoprecipitates. As displayed in figure 8, these *a*–*b* plane defects do not appear to truncate the BZO nanocolumns, contrary to that observed in figure 4.

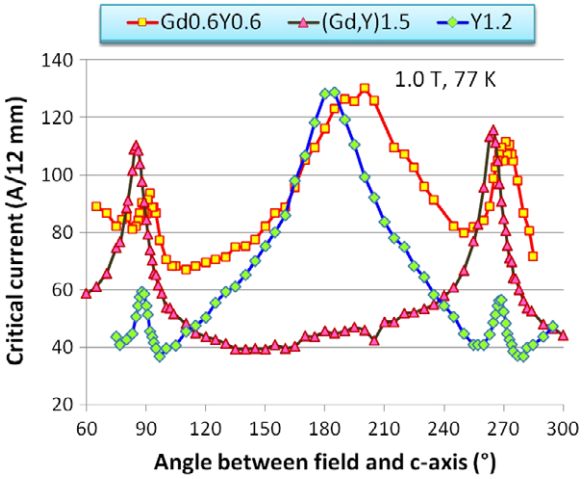

Figure 9. Comparison of angular dependence of 77 K, 1 T critical current density of three 7.5% Zr-doped (Gd, Y)BCO superconducting tapes made with different amounts of Gd and Y in the precursor.

Hence these nanocolumns are found to extend over long lengths perpendicular to the film plane and are likely pin vortex lines along the *c*-axis over a significant length and lead to high critical current when the magnetic field is applied along the *c*-axis. The low critical current in the magnetic field orientation along the *a–b* plane in samples with low Gd and high Y content, such as the $Gd_{0.2}Y_{1.0}$ film, implies that the *a–b* plane defects seen in figure 8 are not strong pinning centers, at least at 77 K in low magnetic fields.

The remarkable differences in the angular dependence of critical current of samples with the same 7.5% Zr doping but with different rare-earth combinations are summarized in figure 9. The figure displays the critical current behavior of $Gd_{0.6}Y_{0.6}$, $Gd_{0.0}Y_{1.2}$, and $Gd_{0.75}Y_{0.75}$ films. The first two films were 0.7 μm thick and the third was 0.5 μm thick. In spite of the same level of Zr doping in all three samples, substantial differences are seen. The $Gd_{0.6}Y_{0.6}$ film exhibits strong peaks in critical current in orientations of field both parallel and perpendicular to the film plane, whereas the $Gd_{0.0}Y_{1.2}$ shows a comparable peak in critical current in the orientation of field perpendicular to the film plane but an extremely weak film in the parallel orientation. On the other hand, the $Gd_{0.75}Y_{0.75}$ film reveals a strong peak in the orientation parallel to the film plane but no peak at all in the perpendicular orientation. It is clear that the in-field performance of Zr-doped films can be significantly manipulated by the content and type of rare-earth employed. Additionally, potential substitution of Ba by Gd in (Gd, Y)BCO films could impact flux pinning characteristics.

4. Summary

The influence of rare-earth type and rare-earth content in (Gd, Y)BCO films made by MOCVD on IBAD templates on metal substrates has been studied for a constant Zr-doping level of 7.5% in the precursor. Critical currents of the films were measured at 77 K in magnetic fields up to 1.5 T. Films with increasing rare-earth content, and constant Gd:Y value, show systematically increasing critical currents with the magnetic field orientation parallel to the film plane and systematically decreasing critical currents with the field perpendicular to the film plane. BZO nanocolumns along the *c*-axis are observed in all samples but the amount of RE_2O_3 nanoprecipitates along the *a–b* plane are found to increase with increasing rare-earth content. These nanoprecipitates are found to truncate the growth of BZO nanocolumns, which is believed to be the reason for the trends in critical current observed with increasing rare-earth content. A second set of samples with varying ratio of Gd:Y and a constant total rare-earth content were fabricated with a fixed Zr-doping value of 7.5%. In this set of samples, the zero-field critical currents of all samples were found to be nearly the same, but the in-field performance displayed significant variations. Samples with low Gd and high Y content were found to exhibit a decreasing trend in critical current in the magnetic field orientation parallel to the *a–b* plane. On the other hand, the critical current values of all samples were found to be nearly identical in the magnetic field orientation perpendicular plane. Microstructure analysis of low Gd, high Y content samples exhibited elongated BZO nanocolumns without significant disruption by defects along the *a–b* plane. In summary, findings from this work show that rare-earth content and type substantially affect the critical currents of Zr-doped thin film superconducting tapes in the presence of a magnetic field at 77 K even if the Zr content is unchanged. This finding opens up an opportunity to choose the appropriate rare-earth type and content to maximize the benefit of Zr doping in REBCO superconducting tapes. It needs to be determined whether the trends observed in this work would extend to low temperature and high magnetic fields.

Acknowledgments

The work at the University of Houston and SuperPower was partially supported by the US Department of Energy. The research at the Electron Microscopy Center at Argonne National Laboratory is supported by the USDOE, Office of Science, Office of Basic Energy Sciences under contract DE-AC02-06CH11357 between U. Chicago Argonne, LLC, and the USDOE.

References

[1] Selvamanickam V *et al* 2009 High performance 2G wires: from R & D to pilot-scale manufacturing *IEEE Trans. Appl. Supercond.* **19** 3225–30

[2] Kakimoto K *et al* 2010 High-speed deposition of high-quality RE123 films by a PLD system with hot-wall heating *Supercond. Sci. Technol.* **23** 014016

[3] Rupich M W *et al* 2010 Advances in second generation high temperature superconducting wire manufacturing and R & D at American Superconductor Corporation *Supercond. Sci. Technol.* **23** 014015

[4] Foltyn S R, Wang H, Civale L, Jia Q X, Arendt P N, Maiorov B, Li Y, Maley M P and MacManus-Driscoll J L 2005 Overcoming the barrier to 1000 A/cm width superconducting coatings *Appl. Phys. Lett.* **87** 162505

[5] Selvamanickam V, Chen Y, Xie J, Zhang Y, Guevara A, Kesgin I, Majkic G and Martchevsky M 2009 Influence of Zr and Ce doping on electromagnetic properties of (Gd, Y)–Ba–Cu–O superconducting tapes fabricated by metal organic chemical vapor deposition *Physica* C **469** 2037–43

[6] Chen Y, Selvamanickam V, Zhang Y, Zuev Y, Cantoni C, Specht E, Paranthaman M P, Aytug T, Goyal A and Lee D 2009 Enhanced flux pinning by $BaZrO_3$ and $(Gd, Y)_2O_3$ nanostructures in metal organic chemical vapor deposited GdYBCO high temperature superconductor tapes *Appl. Phys. Lett.* **94** 062513

[7] MacManus-Driscoll J L, Foltyn S R, Jia Q X, Wang H, Serquis A, Civale L, Maiorov B, Hawley M E, Maley M P and Peterson D E 2004 Strongly enhanced current densities in superconducting coated conductors of $YBa_2Cu_3O_{7-x} + BaZrO_3$ *Nature Mater.* **3** 439–43

[8] Kang S *et al* 2006 High-performance high-T_c superconducting wires *Science* **311** 1911–4

[9] Yamada Y *et al* 2005 Epitaxial nanostructure and defects effective for pinning in $Y(RE)Ba_2Cu_3O_{7-x}$ coated conductors *Appl. Phys. Lett.* **87** 132502

[10] Matsumoto K and Mele P 2010 Artificial pinning center technology to enhance vortex pinning in YBCO coated conductors *Supercond. Sci. Technol.* **23** 014001

[11] Gutiérrez J *et al* 2007 Strong isotropic flux pinning in solution-derived $YBa_2Cu_3O_{7-x}$ nanocomposite superconductor films *Nature Mater.* **6** 367–73

[12] Varanasi C, Burke J, Wang H, Lee J H and Barnes P 2008 Thick $YBa_2Cu_3O_{7-x} + BaSnO_3$ films with enhanced critical current density at high magnetic fields *Appl. Phys. Lett.* **93** 092501

[13] Harrington S A, Durrell J H, Maiorov B, Wang H, Wimbush S C, Kursumovic A, Lee J H and MacManus-Driscoll J L 2009 Self-assembled, rare earth tantalate pyrochlore nanoparticles for superior flux pinning in $YBa_2Cu_3O_{7-\delta}$ films *Supercond. Sci. Technol.* **22** 022001

[14] Feldmann D M, Holesinger T G, Maiorov B, Foltyn S R, Coulter J Y and Apodaca I 2010 Improved flux pinning in $YBa_2Cu_3O_7$ with nanorods of the double perovskite Ba_2YNbO_6 *Supercond. Sci. Technol.* **23** 095004

[15] Wee S H, Goyal A, Zuev Y L, Cantoni C, Selvamanickam V and Specht E D 2010 Formation of self-assembled, double-perovskite, Ba_2YNbO_6 nanocolumns and their contribution to flux-pinning and J_c in Nb-doped $YBa_2Cu_3O_{7-\delta}$ films *Appl. Phys. Express* **3** 023101

[16] Selvamanickam V, Xie Y, Reeves J and Chen Y 2004 MOCVD-based YBCO-coated conductors *MRS Bull.* **29** 579–82

[17] Arendt P N and Foltyn S R 2004 Biaxially textured templates for conductors *MRS Bull.* **29** 543–50

[18] Xiong X, Kim S, Zdun K, Sambandam S, Rar A, Lenseth K P and Selvamanickam V 2009 Progress in high throughput processing of long-length, high quality, and low cost IBAD MgO buffer tapes at SuperPower *IEEE Trans. Appl. Supercond.* **19** 3319–22

[19] Maiorov B, Gibbons B J, Kreiskott S, Matias V, Jia Q X, Holesinger T G and Civale L 2005 Influence of tilted geometries on critical current in superconducting thin films *IEEE Trans. Appl. Supercond.* **15** 2582–5